Tailoring ZIF-67 Carbonization: A Comprehensive Study on Structural, Morphological and Electrochemical Properties for Dual Dopamine and Uric Acid Detection

Vidyagouri Karkal[a], Rupali Mane[b], Neetu Jha[b*]

a – Centre of Green Technology, Institute of Chemical Technology, Nathalal Parekh Marg, Mumbai - 400019. India.

b – Department of Physics, Institute of Chemical Technology, Nathalal Parekh Marg, Mumbai - 400019. India.

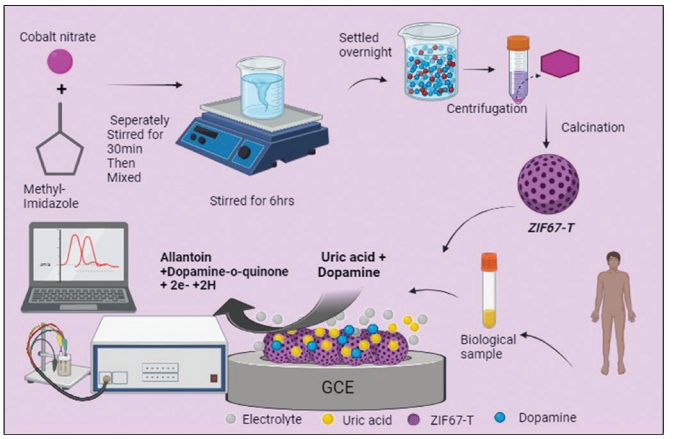
*Corresponding Author

Email: nr.jha@ictmumbai.edu.in

Abstract

This work presents the optimization of pyrolysis temperature for Co-based Zeolite Imidazole Frameworks (ZIF67) and its application as a nonenzymatic electrochemical sensor for the simultaneous detection of dopamine and uric acid. The pyrolysis process was meticulously conducted across a range of temperatures. Structural, morphological and surface area properties of ZIF67 and its carbonized derivatives were investigated through X-ray diffraction (XRD), scanning electron microscopy (SEM) and BET N_2 absorption-desorption studies. To evaluate the performance of the synthesized materials performance for sensing application, comprehensive electrochemical analyses were conducted employing cyclic voltammetry (CV) and differential pulse voltammetry (DPV). The investigation revealed that ZIF67, carbonized at 800°C exhibited superior electrocatalytic activity compared to the other carbonized ZIF67 derivatives. In conclusion, this study underscores the significance of carbonization in enhancing the electrocatalytic properties of ZIF-67 based materials. The results demonstrates that ZIF67-800 as a promising candidate for such applications, exhibiting remarkable electrocatalytic activity, wide linear detection range, low detection limits, and excellent selectivity and stability in biological samples. These findings highlight its potential for practical applications in simultaneous dopamine and uric acid detection.

Keywords: *Electrochemical sensors, simultaneous detection, Metal organic framework, Temperature optimization, Differential pulse voltammetry, Cyclic Voltammetry, human plasma*



Graphical Abstract

1. Introduction

Dopamine, a neurotransmitter, plays a crucial role in numerous physiological and cognitive functions within the human brain. It is often referred to as 'feel-good' chemical due to its contributions in regulating emotions, motivation, pleasure, and reward. Dopamine functions as a chemical messenger, facilitating signal transmission between neurons and influencing information exchange across various brain regions. This neurotransmitter is vital for processes such as coordinating movement, learning and memory, attention, and maintaining hormonal balance[1]. The dysregulation of dopamine has been linked to various neurological and psychiatric disorders, including Parkinson's disease, schizophrenia, addiction, and depression. A comprehensive understanding of opamine's intricate mechanisms and roles is essential for advancing our knowledge of brain function and developing target treatments for neurological and psychiatric conditions. In general, the concentration

of dopamine in the brain is relatively low compared to other neurotransmitters. Estimates suggest that dopamine levels in the human brain typically range from approximately 0.1 to 0.3 micromoles per liter (μmol/L). However, these concentrations can vary significantly based on specific brain regions and the individual's physiological state[2].

Uric acid (UA), also known as 2,4,8 - Trihydroxypurine, serves as the final product of purine metabolism, encompassing adenine and guanine. In humans, the absence of the urate enzyme gene prevents the breakdown of uric acid, leading to its accumulation in the body. Elevated uric acid levels can lead to various diseases related to acid level fluctuations, such as gout, neurological disorders, cardiovascular issues, arthritis, and kidney diseases. Typically, the average uric acid concentration in the blood of a healthy individual ranges from 236 to 420 μmol/L. Elevated uric acid levels known as hyperuricemia, are linked to conditions like gout. Uric acid also functions as a biomarker for cardiovascular diseases, hypertension, metabolic syndrome, and diabetes[3].

Rapid development in the health care and point of care device development necessitates the creation of low-cost flexible, innovative and user friendly sensors. Conventional analytical methods, including spectroscopy[4], HPLC[5], fluorescence method[6] and colorimetry[7] have been employed for dopamine and uric acid detection but possess disadvantages such as high cost, reliance on sophisticated instruments, complex operational procedures, time consuming sample preparation and limited on-site monitoring capabilities. Consequently, there is a growing need for the development of simple, highly sensitivity, selective, real time and cost effective sensor[8].

Electrochemical sensors offer several advantages, including affordability, simplicity, high sensitivity, and rapid real-time detection. They can be employed in both enzymatic and non-enzymatic configurations[9]. Enzymatic sensors, however, have significant drawbacks, including the high cost of enzymes, limited reproducibility, challenges in immobilization, and the need for precise control of operational parameters such as pH and temperature. On the other hand, non-enzymatic sensors demonstrate superior performance, particularly when electrodes are modified with nanomaterials to enhance electron-species interaction and peak separation[10]. In non-enzymatic approaches, analyte oxidation occurs at the surface of modified electrodes. Various nanomaterials are utilized for electrode modification, including carbon-based materials such as carbon nanotubes (CNTs), graphene, graphene oxides, fullerenes, and carbon dots[11]. Inorganic nanomaterials encompass metals and metal oxides [12] while organic nanomaterials include dendrimers, micelles, liposomes, and polymers[13]. Additionally, composite materials with multiphase nanoparticles or complex structures, such as hybrid nanofibers and metal-organic frameworks [14] [15] are also employed in sensor development.

Metal-Organic Frameworks (MOFs) represent a class of hybrid porous materials with diverse applications in catalysis, gas storage, batteries, gas separation, and electrochemical sensors. Their utilization in electrochemical sensors has yielded notable benefits, including improved electrocatalytic performance, adaptable stereochemistry, and high chemical stability. MOFs offer advantages such as rapid mass transfer and ample active sites, enhancing their electrocatalytic activity. They also possess a high surface area while maintaining low density[16]. Within the MOF family, Zeolite Imidazole Frameworks (ZIFs) stand out as a subclass. An example is ZIF-67, composed of cobalt ions and 2-methylimidazole. ZIFs exhibit exceptional porosity, a large surface area, and active sites conducive to redox reactions. However, they do have drawbacks, notably poor stability and low electrical conductivity. These limitations can be addressed through the pyrolysis of materials[17],[18]

This study focuses on the simultaneous electrochemical detection of dopamine and uric acid using a glassy carbon electrode (GCE) modified with ZIF67 and compares it with carbonized ZIF67 at various temperatures. ZIF67 was subjected to carbonization within the temperature range of 500

to 900ºC to determine the optimal temperature for enhanced conductivity and stability. Altering the temperature resulted in improvements in the electronic structure, charge, and spin density of atoms, thereby reducing energy barriers and facilitating smoother electron transfer processes. The high surface area achieved after pyrolysis of ZIF67 enabled efficient oxidation of both dopamine and uric acid. Acid treatment was applied to ZIF67 to eliminate inactive species and promote the formation of an atomically dispersed network. The modified electrode exhibited excellent selectivity, sensitivity, and a wide linear detection range. This proposed method was successfully applied to the analysis of real samples, yielding satisfactory results.

2. Experimental

Materials

We sourced Cobalt nitrate hexahydrate, 2-methyl imidazole, polyvinyl pyridine, methanol, uric acid (UA), dopamine (DP), Potassium ferrocyanide, and potassium chloride from SD Finechem Ltd. To prepare a 0.1M Potassium Phosphate Buffer, we used Potassium Dihydrogen Phosphate and Dipotassium hydrogen phosphate, adjusting the pH to various values using Phosphoric acid (H3PO4) and Sodium hydroxide (NaOH). All the reagents utilized were of analytical grade, and we conducted all experiments using double-distilled water.

Instrumentation

A comprehensive array of analytical techniques was employed to investigate various aspects of the materials, including their synthesis, structure, morphology, chemical bonding, interfacial behavior, and effective surface area. To determine elemental composition and examine crystal structure, X-ray diffraction (XRD) spectroscopy was utilized, employing a Rigaku Ultima IV machine with CuKα radiation. Scanning electron microscopy (SEM), using a ZEISS Gemini SEM system, was employed for morphological studies. Fourier-transform infrared spectroscopy (FTIR) was employed to confirm chemical bonding with a L1600300 Spectrum Two LITA instrument from Perkins. Surface area and pore size were determined through Brunauer-Emmett-Teller (BET) analysis. To evaluate the interfacial behavior and effective surface area of various electrodes, electrochemical impedance spectroscopy, differential pulse voltammetry, and cyclic voltammetry were performed using a Metrohm (PGSTAT204) electrochemical workstation. Finally, the material's surface area and pore size were determined through BET analysis using a Porous Material Inc. BET-201A instrument, with N2 adsorption-desorption isotherms measured at 77K.

Preparation of ZIF67 and ZIF67-T

To synthesize ZIF67, 0.49g of Cobalt nitrate was dissolved in 20 ml of methanol, and separately, 1.25g of 2-methyl imidazole was dissolved in 20 ml of methanol. Each solution was stirred for 30 minutes. The solution containing cobalt salts was slowly added to the solution containing 2-methyl imidazole. This addition caused the color to change from colorless to purple, attributed to the introduction of the initially pink-colored Co ion solution. The resulting mixture was continuously stirred for 6 hours. After this period, the solution was left undisturbed overnight. The sediment was washed three times using methanol at 6000 rpm for 10 minutes. The resulting pellet was dried to obtain ZIF67. Subsequently, ZIF67 underwent carbonization in a tube furnace under varying temperatures in a nitrogen atmosphere. Each temperature was maintained for 1.5 hours before cooling to room temperature. The resulting samples were designated as ZIF67-500, ZIF67-600, ZIF67-700, ZIF67-800, and ZIF67-900.

Pyrolysis of ZIF led to the oxidation of volatile elements such as C, N, and H into gaseous by-products. These gases created porous, N-doped ZIF-derived metal with interconnected pores. All samples then underwent acid leaching using 0.1M HCL and were left overnight to remove any unreacted Co species, further enhancing porosity. The settled materials were subsequently centrifuged using distilled water until a neutral pH was achieved before being dried.

Electrochemical measurements

Samples of weight, 5 mg were dissolved in 1 ml of N, N-Dimethylformamide, and these slurries were then subjected to ultrasonication for 15 minutes to achieve a well-dispersed solution. Subsequently, a glassy carbon electrode (GCE) was polished using an alumina solution, and 10μL of this prepared solution was applied to the GCE and allowed to dry. The Differential Pulse Voltammetry (DPV) and Cyclic Voltammetry (CV) experiments were conducted in a phosphate buffer with a pH of 6, containing appropriate concentrations of DP (dopamine) and UA (uric acid). DPV measurements were recorded over a potential range spanning from -0.2V to +0.6V, using a pulse amplitude of 50mV and a pulse width of 50ms in the phosphate buffer. The electrode underwent potential cycling between -0.2V and 0.6V in the same phosphate buffer at a scan rate of 100mV/s until a steady state was achieved for subsequent experiments. The electrochemical behaviors of the electrodes were investigated using Electrochemical Impedance Spectroscopy (EIS) in a solution containing 5.0mM Fe $(CN)_6^{3-/4-}$ and 0.1M KCL with a frequency range between 0.1 and 10kHz. All electrochemical experiments were carried out at room temperature.

Sample analysis

Human plasma samples were generously provided by healthy volunteers. For analysis, 1 mL of each human plasma sample was diluted by a factor of 50 with phosphate buffer and subsequently analyzed using Differential Pulse Voltammetry (DPV). The recorded data included the peak currents of the analytes.

3. Result and discussion

Choice of materials

ZIF67 exhibits a large surface area and nano-porous structure, making it an ideal oxidation site for electrochemical reactions involving dopamine and uric acid. This unique structure contributes to the high current response observed for both DP and UA. Pyrolysis of ZIF67 at various temperatures enhances its surface area, chemical stability, and flexibility. Additionally, it improves the material's conductivity. During pyrolysis, the graphitic degree of the resulting samples increases with higher applied temperatures, albeit with a gradual decrease in surface area. ZIF67 contains Co species that transform into metallic Co nanoparticles during carbonization. These Co nanoparticles can act as catalysts for the graphitization of carbon. The electrochemical response for detecting DA and UA is significantly influenced by the degree of graphitization of carbon, which is why it was chosen as the platform for the determination of DP and UA.

Material Characterization of ZIF67-T

The prepared samples, including ZIF67, ZIF67-500, ZIF67-600, ZIF67-700, ZIF67-800, and ZIF67-900, were characterized for structure, functional groups, morphology and surface area using techniques XRD, FTIR, SEM, and BET, respectively. The XRD patterns, presented in Fig 1A, demonstrated that all the peaks are aligned perfectly with the standard simulated pattern of ZIF67, indicating the absence of impurities[19]. Fig 1B illustrates that all the samples underwent structural transformations after carbonization. As the temperature increased up to 900°C, the diffraction peak around 25°, corresponding to the carbon (002) interlayer, became more distinct and intense, signifying the development of highly graphitized carbon. However, the (111) and (200) diffractions of the Co crystal at 44.2° and 51.6°, respectively, were still observable, suggesting the presence of some Co nanoparticles even after acid treatment. SEM images (Fig 1C) revealed that the polyhedral morphology of ZIF67 with particle sizes ranging from 1 to 2 μm. Post carbonization, Co species aggregates leading to the formation of metallic nanoparticles[20]. SEM images of ZIF67 after pyrolysis at 800 °C are shown in Fig 1D. This confirms highly porous structure of ZIF67-800, which also leads to increase in surface area. The overall particle shape and size of the original ZIF67 precursor were preserved, but a higher degree of distortion was observed due to pyrolysis [21].

For the investigation of the surface area and porosity of the catalyst, N_2 absorption-desorption and Barrett-Joyner-Halenda (BJH) measurements were conducted. Notably, the surface area of the catalyst increased as the pyrolysis temperature increased. The surface area values for ZIF67-600, ZIF67-700, ZIF67-800, and ZIF67-900 were obtained to be 290, 410, 471, and 530 m^2/g, respectively (Fig 1E). This

increase in surface area with temperature can be attributed to two factors: post-acid treatment, which removed agglomerated and unreacted Co atoms embedded in the carbon system, and the presence of micropores. The average pore size for ZIF67 was 1.69 nm, which decreased to 1.26 nm after pyrolysis at 600°C. At 700°C, the pore size increased to 1.28 nm, further expanding to 1.49 nm at 800°C, and then returning to 1.28 nm at 900°C. These micropores contribute to improved mass transport and provide a high density of active Co sites. However, it was observed that ZIF67-800 exhibited a larger pore size than ZIF67-900, possibly due to structural defects. At high temperatures, the material tends to expose more metallic Co, forming closed and unresolved graphitic shells that hinders the access of N_2 molecule [22].

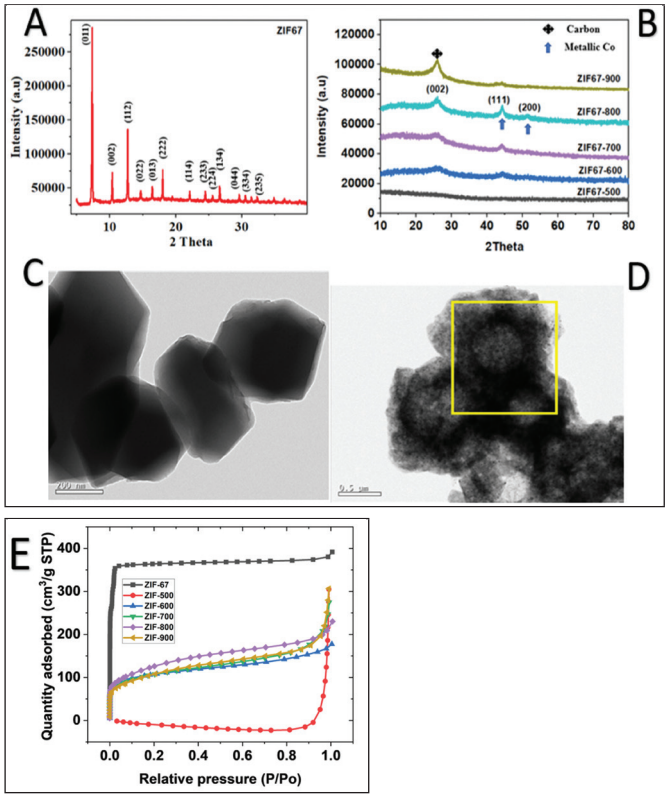


Fig 1A. XRD spectra of pure ZIF67, 3B. XRD spectra of all carbonized ZIF67, 3C. SEM images of ZIF67-800, 3D. High resolution SEM image of ZIF67-800, 3E. N_2 absorption-desorption isotherms of all the ZIF67 materials

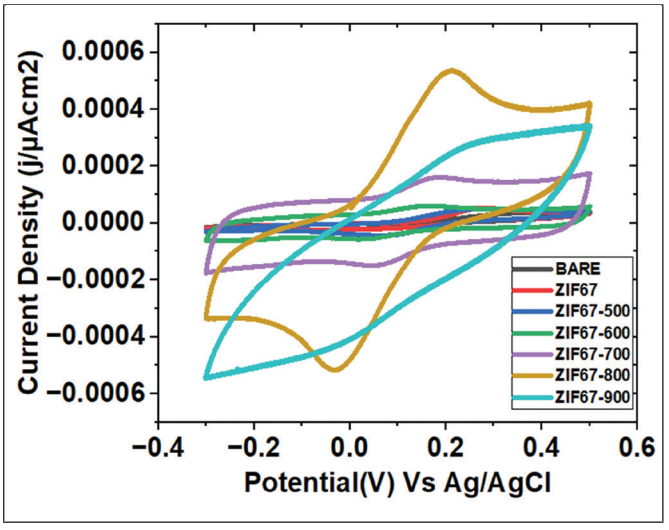
Electrochemical Characterization of modified electrodes

The electrochemical properties of various electrodes were studied using $K_3[Fe(CN)_6]$ as a probe via cyclic voltammetry. In Fig 2A, cyclic voltammograms of the bare Glassy Carbon Electrode (GCE), ZIF67, ZIF67-500, ZIF67-600, ZIF67-700, ZIF67-800, and ZIF67-900 in a solution containing 5.0 mM $[Fe(CN)_6]^{3-/4-}$ and 0.1 M KCl are presented. The anodic peak current (Ipa) obtained with ZIF67-800 was at much higher current density compared to other electrodes. This is attributed to its larger surface area and enhanced conductivity of the modified electrode.

For a reversible process, the peak current (I_{pa}) is linearly proportional to the square root of the scan rate ($v_{1/2}$), as described by the Randles-Sevcik formula:

$$I_{pa} = 2.69\times10^5 n^{3/2} A D^{1/2} C v^{1/2}$$

Where I_{pa} is the peak current, n is the number of electrons involved (n=1), A is the surface area of electrode, C is the concentration of the reactant in electrolyte. D is the diffusion coefficient of the $[Fe(CN)_6]^{3-/4-}$ and v is the scan rate. Thus, from the slope of the anodic peak current (I_{pa}) vs square root of scan rate($v^{1/2}$) relation, the value of A for ZIF67-800 was obtained and was found to be much larger than that of non-pyrolyzed ZIF67 and bare GCE. This indicates increase in electroactive surface area of the modified electrode due to the pyrolysis of ZIF67 at high temperature. Electrochemical effective surface area of bare GC, ZIF67, ZIF67-500, ZIF67-600, ZIF67-700, ZIF67-800, ZIF67- 900 are 0.3166 m², 0.478 m², 0.368 m²,0.688 m², 1.982 m², 4.990 m² and 3.651 m² respectively.



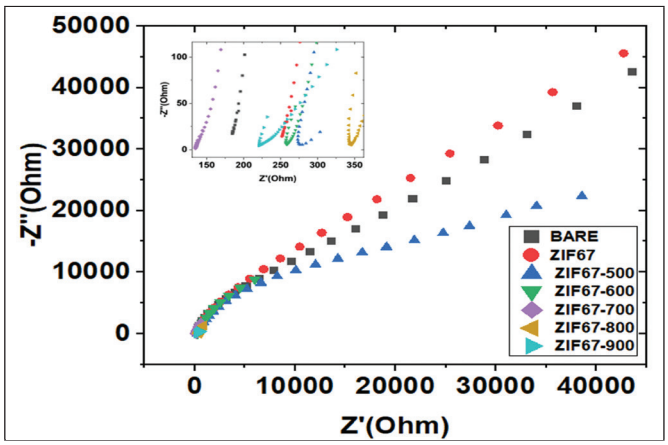


Fig 2 Electrochemical Charcterization of bare GCE, ZIF67, ZIF67-500, ZIF67-600, ZIF67-700, ZIF67-800 and ZIF67-900 in 5.0 mM $[Fe(CN)_6]^{3-/4-}$ containing 0.1 M KCl(A)Cyclic Voltametry B) Electrochemical impedance spectroscopy to determine the x-intercept for R_{ct}(shown in the inset)

Electrochemical Impedance Spectroscopy (EIS) was performed and data shown in Fig 2B, to investigate the electronic charge properties of the modified electrodes, using the redox couple probe $[Fe(CN)6]^{3-/4}$ in the solution of 5mM $Fe(CN)_6^{3-/4-}$ containing 0.1 M KCL, as shown in the Fig 5. The diameter of semicircle element at higher frequencies corresponded to the electron transfer resistance (R_{ct}) between electrode surface and $[Fe(CN)_6]^{3-/4-}$, while the linear part at lower frequency represents the diffusion driven process. The Nyquist curve of the bare GCE displayed a semicircle in the high-frequency region. After introducing ZIF67, the diameter of the semicircle increased, indicating modification with the initially poorly conductive ZIF67. However, the diameter of the semicircle decreased for ZIF67-800 and ZIF67-900 due to their high electrical conductivity. The semicircle was smallest when ZIF67-800 and ZIF67-900 were used as electrode material, which can be attributed to the graphitization of carbon. This suggests that the poor conductivity of ZIF67 was overcome by carbonization, indicating high interfacial electron transfer for ZIF67-800 and ZIF67-900.

Electrochemical behavior of DP and UA

The electrochemical behaviors of dopamine (DP) and uric acid (UA) for different electrode materials were investigated in phosphate buffer at pH 6 using cyclic voltammetry and differential pulse voltammetry. Fig 3, shows the cyclic voltamtery curve obtained for ZIF67 based materials obtained at the scan rate of 100 mV/s. A small oxidation peak was observed for DP at the bare Glassy Carbon Electrode (GCE). However, when ZIF67 was employed, the current density increased significantly indicating superior electrocatalytic activity and fast electron transfer for DP at 0.01V vs Ag/AgCl. Upon the introduction of carbonized ZIF67, a substantial increase in the oxidation peak current was observed, attributed to the greater surface area and porosity along with high conductivity of ZIF-T. Notably, ZIF67-800 displayed the highest oxidation peak current, suggesting enhanced DP oxidation due to the synergistic effect of ZIF67's porosity and the superior conductivity of graphitic carbon formed after carbonization. Furthermore, ZIF67-800/GCE shifted the oxidation peak potential for DP and UA to less negative values, accompanied by a significant increase in current density. Specifically, for DP, the shift was observed from 0.2V to 0.01V, and for UA, it shifted from 0.31V to 0.18V. Fig 6 also reveals two well-defined oxidation peaks corresponding to DP and UA in mixtures of both compounds. The oxidation peak currents for DP and UA were significantly higher for ZIF67-800 than those obtained with other electrode materials[23]. For ZIF67-800, the peak potential for DP was observed at 0.01V with a current response of 0.28 mA/cm^2, and similarly, for UA, the peak potential was observed at 0.18V with a current response of 0.39mA/cm^2. The distinct electrochemical signals at the ZIF67-800/GCE electrode provide a favorable opportunity for the effective and simultaneous determination of DP and UA in phosphate buffer.

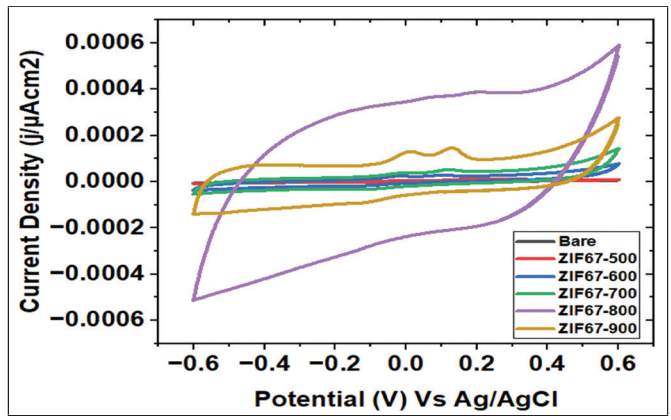


Fig 3 Cyclic Voltammetry results of all materials in presence of 100M concentration of DP and UA with a scan rate of 100mV/s

Simultaneous determination of DP and UA

In order to achieve the optimum electrochemical results using DPV, pH and scan rates were optimized to pH- 6 and scan rate to 10mV.s^{-1}. The simultaneous determination of DP and UA for all the carbonized materials were studied using DPV and shown in Fig 4. DPVs were recorded for various concentrations of DP and UA from 10 to 500µM. Fig 4A, shows DPV curves of DP and UA in mixture solution by simultaneously changing their concentrations. The peak current (I_{pa}) were proportional to their concentration from 10 µM to 500 µM for DP and from 10 µM to 500 µM for UA. The regression equation utilized was I_{pa}(µA.cm^{-2}) = 0.9673C(µM) (R=0.98) for DP and I_{pa}(µA.cm^{-2}) = 0.107C(µM)-(R=0.98) for UA, respectively. The detection limit (LOD) for DP and UA were estimated to be 23.3µM and 17.8µM (S/N=3), respectively. The sensitivity for DP and UA were 1999.3 µA. µM^{-2}cm^{-2} and 1069.3 µA. µM^{-2}cm^{-2}, respectively. Comparing the data for the simultaneous and quantitative determination DP and UA, ZIF67-800/GCE shows best performance as expected sue to its high current sensitivity and good resolution.

Fig 4B, shows DPV data with variation in concentration of DP, where UA was maintained at constant concentration of 100 µM. The peak current of DP was found to be proportional to the concentration, which was varied from 10 µM to 500 µM (R=0.97). The regression equation of I_{pa}(µA.cm^{-2})=0.116C(µM) – (R=0.98) was followed with the sensitivity of 1569 µA.µM^{-2}.cm^{-2}. Similar patterns were observed for UA with respect to DP at a constant concentration of 100 µM as shown in the fig 4C, the peak current of UA was proportional to the concentration from 10 µM–500 µM (R=0.98) with a regression equation of Ipa(µA. cm^{-2})=0.073(µM)–(R=0.98), sensitivity was 1009 µA.µM^{-2}.cm^{-2}, indicating that the oxidation of DP and UA at ZIF67-800 modified electrode took place independently without any mutual interference.

These results indicate that ZIF67-800/GCE can be effectively employed for the simultaneous determination of dopamine (DP) and uric acid (UA) without interference between the two analytes. Table 1 provides a summary comparing ZIF67-800 modified electrodes with other carbonized modified electrodes for the simultaneous detection of DP and UA. The table illustrates that the modified electrode developed in this study exhibits a low detection limit and a wide linear range. The improved electrocatalytic performance of ZIF67-800/GCE can be attributed to its highly porous structures with a high degree of graphitization, improving the electronic conductivity. Graphitic nitrogen doped porous carbon structures are known for their high electrochemical performances.

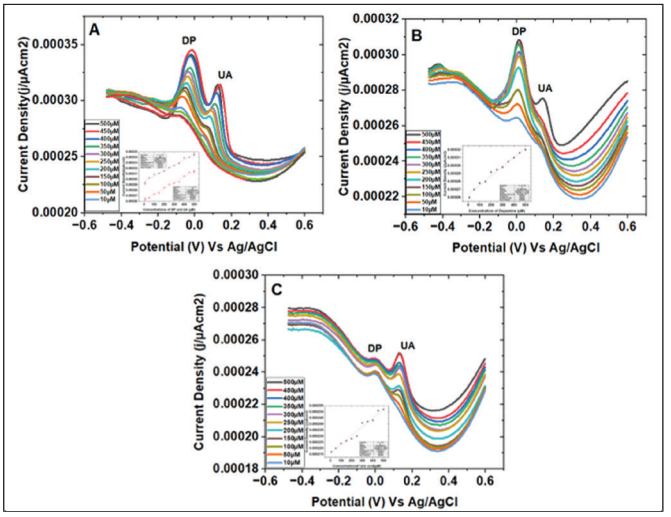


Fig 4A DPV cures for Simultaneous detection of DP and UA at different concentration, B) DPV curves for detection of DP with concentration of UA as constant and C)DPV curves for detection of UA with concentration of DP as constant

Table 1) Comprehensive comparison of developed ZIF67-T materials for the simultaneous detection of DP and UA

Materials	Linear range(µM)		Detection limit (µM)		Sensitivity (µA. µM^{-2}.cm^{-2})	
	DP	UA	DP	UA	DP	UA
ZIF67-500	50-1000	50-1000	49.1	40.3	488.9	217.8
ZIF67-600	50-1000	50-1000	44.9	45.3	699.33	500.3
ZIF67-700	50-1000	30-1000	35.5	25.3	747.4	899.7
ZIF67-800	10-1000	10-1000	23.3	5.3	1999.8	1069.4
ZIF67-900	50-1000	40-1000	49.2	25.9	680.3	789.3

Mechanism

When a sample containing both dopamine and uric acid is introduced to the modified electrode, both analytes can be simultaneously detected through their distinct electrochemical signals. The modified electrode facilitates the oxidation of dopamine, resulting in an oxidation peak in the current-voltage curve at 0.01V. Uric acid also undergoes oxidation, but at a different potential of 0.18V compared to dopamine. This selective detection of uric acid leads to a separate oxidation peak in the current-voltage curve, with its peak potential and current intensity being characteristic of uric acid. Fig 5 illustrates the mechanism of simultaneous detection of dopamine and uric acid on the modified electrode surface. To establish the linear range, a series of standard solutions with known analyte concentrations are prepared. Sensor is then employed to measure the current response at each concentration. By plotting the response against concentration, the linear range is determined by identifying the range of concentrations exhibiting a linear relationship. The Limit of Detection (LOD) can be calculated as the concentration corresponding to a certain multiple of the standard deviation of the blank signal divided by the slope of the calibration curve. Sensitivity is calculated as the slope of the calibration curve, obtained through linear regression fitting of the experimental data points.

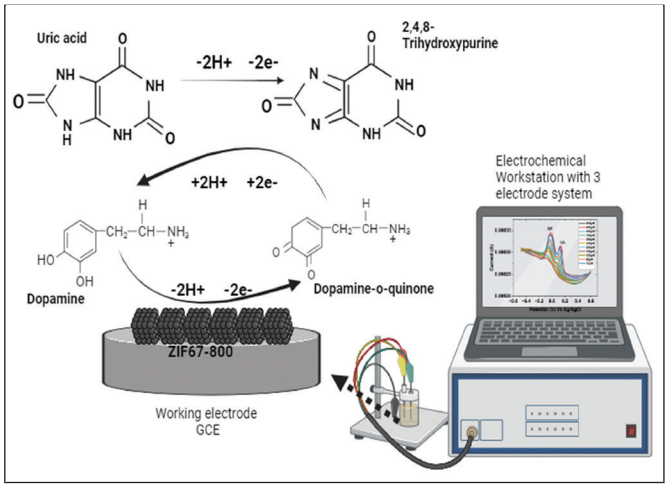
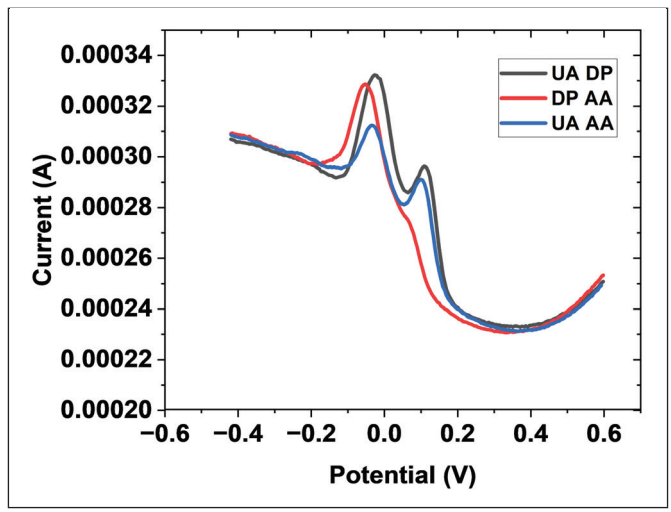


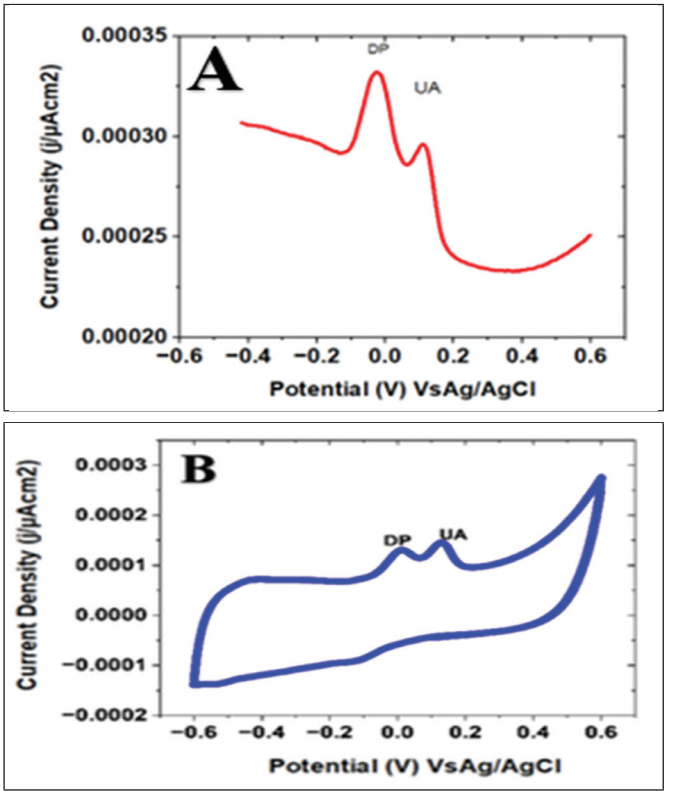
Fig 5 Mechanism of simultaneous detection of dopamine and uric acid on the surface of modified electrode

Selectivity, stability and reproducibility

Resistance to interference is a crucial parameter for an electrochemical sensor. Ascorbic acid (AA), which is a major interfering species affecting the electrochemical detection of dopamine (DP) and uric acid (UA) in the analysis of real samples, was tested at high concentrations. Fig 6A, depicts the interference of DP on the oxidation of AA. It exhibited a poor electrochemical response on ZIF-T and the separation of the oxidation peak potentials of DP and UA was significant enough for clear distinction. This may be attributed to electrostatic repulsion caused by the negatively charged carboxylate groups on the graphitic carbon, which exclude most of the AA anions from the electrode surface. Fig 6B demonstrates the insignificant interferences observed for several compounds, including AA, glucose, urea, hydrogen peroxide, and ethanol. The Differential Pulse Voltammetry (DPV) curve for these interfering species shows no additional peaks. All these results collectively indicate the excellent selectivity of ZIF67-800/GCE.

The stability of ZIF67-800 was assessed (Fig 6C) in a mixed solution containing 100 µM DP and 100 µM UA. The oxidation currents using this method displayed a relative standard deviation (RSD) of 19.0% for DP and 12.2% for UA in seven successive measurements, demonstrating excellent stability. Reproducibility was tested using four different modified electrodes, yielding an RSD of 5.4% for DP and 3.23% for UA. Therefore, ZIF67-800 exhibits good reproducibility along with considerable stability for the simultaneous determination of DP and UA.





Fige 6A DP interfering for AA oxidation on ZIF67-800 (B)Interference studies in presence of AA, glucose, urea, hydrogen peroxide and ethanol and C Stability of ZIF67-800 after 1000cycles

Analytical application

To assess the materials performance in real samples, ZIF67-800 was employed for the determination of dopamine (DP) and uric acid (UA) in human plasma. Differential Pulse Voltammograms (DPVs) of phosphate buffer (pH=6) in both the absence and presence of a human plasma sample are depicted in Fig 7. A significant increase in peak current was observed at a potential of 2.5V, indicating the presence of UA in the sample.

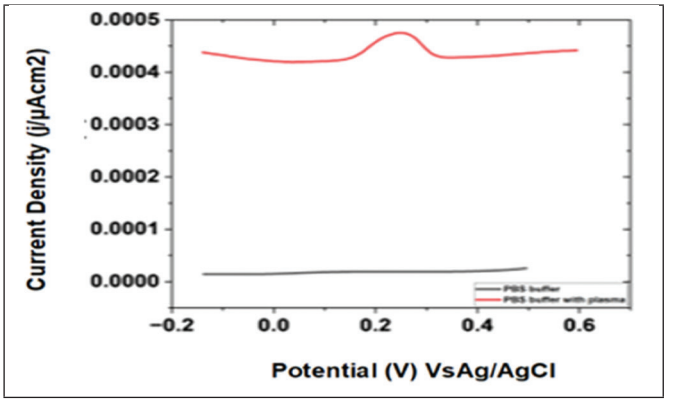


Fig 7 Detection of uric acid in human plasma

Conclusions

In summary, we successfully fabricated a modified glassy carbon electrode by employing a drop-casting technique with ZIF-T. The resulting ZIF67-800-modified electrode exhibited excellent electroactivity for the oxidation of both dopamine (DP) and uric acid (UA). We harnessed this ZIF67-800-modified electrode for the simultaneous determination of DP and UA, and the oxidation peak potentials for these analytes displayed clear distinctions, underscoring its remarkable selectivity and sensitivity. The glassy carbon electrode demonstrated favourable analytical parameters, including a wide linear range and a low detection limit. These attributes can be attributed to the porous structures with a high degree of graphitization, along with the Co nanoparticles acting as catalysts to promote carbon graphitization and facilitate rapid electron transfer. Notably, graphitic carbon structures are known for their higher electrical conductivity compared to amorphous carbon. Furthermore, we successfully applied this glassy carbon electrode to detect DP and UA in human plasma, highlighting its promising potential for real sample analysis.

Acknowledgement

The authors are thankful to the Department of Science and Technology(DST/TMD/HCF/2K18/130) and SERB-Power(SPG/2023/000046) for funding assistance. We would also like to thank SAIF IIT, Bombay for Material Characterization.

References

[1] J. Tang, S. Jiang, Y. Liu, S. Zheng, L. Bai, J. Guo and J. Wang, "Electrochemical determination of dopamine and uric acid using a glassy carbon electrode modified with a composite consisting of a Co(II)-based metalorganic framework (ZIF67) and graphene oxide", Microchimica Acta 185(2018), 486-497, https://doi.org/10.1007/s00604-018-3025-x .

[2] M. U. Anu Prathap and R. Srivastava, "Tailoring properties of polyaniline for simultaneous determination of a quaternary mixture of ascorbic acid, dopamine, uric acid,

and tryptophan," Sensors and Actuators B: Chemical, vol. 177(2013), pp. 239–250, doi: 10.1016/j.snb.2012.10.138.

[3] J. C. Ndamanisha and L. Guo, "Electrochemical determination of uric acid at ordered mesoporous carbon functionalized with ferrocenecarboxylic acid-modified electrode," Biosens Bioelectron, vol. 23(2008), no. 11, pp. 1680–1685, doi: 10.1016/j.bios.2008.01.026.

[4] M. R. Moghadam, S. Dadfarnia, A. M. H. Shabani, and P. Shahbazikhah, "Chemometric-assisted kinetic–spectrophotometric method for simultaneous determination of ascorbic acid, uric acid, and dopamine," *Anal. Biochem.*, vol. 410(2011), no. 2, pp. 289–295, doi: 10.1016/j.ab.2010.11.007.

[5] M. Orts-Arroyo, I. Castro, and J. Martínez-Lillo, "Detection of Hypoxanthine from Inosine and Unusual Hydrolysis of Immunosuppressive Drug Azathioprine through the Formation of a Diruthenium(III) System," *Biosensors*, vol. 11(2021), no. 1, p. 19, doi: 10.3390/bios11010019.

[6] X. Lian and B. Yan, "Phosphonate MOFs Composite as Off–On Fluorescent Sensor for Detecting Purine Metabolite Uric Acid and Diagnosing Hyperuricuria," *Inorg. Chem.*, vol. 56(2017), no. 12, pp. 6802–6808, doi: 10.1021/acs.inorgchem.6b03009.

[7] Y. Tao, Y. Lin, J. Ren, and X. Qu, "A dual fluorometric and colorimetric sensor for dopamine based on BSA-stabilized Aunanoclusters," *Biosens. Bioelectron.*, vol. 42(2013), pp. 41–46, doi: 10.1016/j.bios.2012.10.014.

[8] J. Wang *et al.*, "Dopamine and uric acid electrochemical sensor based on a glassy carbon electrode modified with cubic Pd and reduced graphene oxide nanocomposite," *J. Colloid Interface Sci.*, vol. 497(2017), pp. 172–180, doi: 10.1016/j.jcis.2017.03.011.

[9] G. Wang *et al.*, "Non-enzymatic electrochemical sensing of glucose," *Microchim. Acta*, vol. 180(2013), no. 3–4, pp. 161–186, doi: 10.1007/s00604-012-0923-1.

[10] C. Shan, H. Yang, D. Han, Q. Zhang, A. Ivaska, and L. Niu, "Graphene/AuNPs/chitosan nanocomposites film for glucose biosensing," *Biosens. Bioelectron.*, vol. 25(2010), no. 5, pp. 1070–1074, doi: 10.1016/j.bios.2009.09.024.

[11] L. Zhang, C. Liu, Q. Wang, X. Wang, and S. Wang, "Electrochemical sensor based on an electrode modified with porous graphitic carbon nitride nanosheets (C3N4) embedded in graphene oxide for simultaneous determination of ascorbic acid, dopamine and uric acid," *Microchim. Acta*, vol. 187(2020), no. 2, p. 149, doi: 10.1007/s00604-019-4081-6.

[12] B. Sriram, M. Govindasamy, S.-F. Wang, R. Jothi Ramalingam, H. Al-lohedan, and T. Maiyalagan, "Novel sonochemical synthesis of Fe3O4 nanospheres decorated on highly active reduced graphene oxide nanosheets for sensitive detection of uric acid in biological samples," *Ultrason. Sonochem.*, vol. 58(2019), p. 104618, doi: 10.1016/j.ultsonch.2019.104618.

[13] K. Samoson *et al.*, "Facile fabrication of a flexible laser induced gold nanoparticle/ chitosan/ porous graphene electrode for uric acid detection," *Talanta*, vol. 243(2022), p. 123319, doi: 10.1016/j.talanta.2022.123319.

[14] H. Shu *et al.*, "Single-step electrochemical deposition of high performance Au-graphene nanocomposites for nonenzymatic glucose sensing," *Sens. Actuators B Chem.*, vol. 220(2015), pp. 331–339, doi: 10.1016/j.snb.2015.05.094.

[15] I. Shackery, U. Patil, A. Pezeshki, N. M. Shinde, S. Im, and S. C. Jun, "Enhanced Non-enzymatic amperometric sensing of glucose using Co(OH)2 nanorods deposited on a three dimensional graphene network as an electrode

material," *Microchim. Acta*, vol. 183(2016), no. 8, pp. 2473–2479, doi: 10.1007/s00604-016-1890-8.

[16] N. Kau, G. Jindal, R. Kaur, and S. Rana, "Progress in development of metal organic frameworks for electrochemical sensing of volatile organic compounds," *Results Chem.*, vol. 4(2022), p. 100678, doi: 10.1016/j.rechem.2022.100678.

[17] C. Duan, Y. Yu, and H. Hu, "Recent progress on synthesis of ZIF67-based materials and their application to heterogeneous catalysis," *Green Energy Environ.*, vol. 7(2022), no. 1, pp. 3–15, doi: 10.1016/j.gee.2020.12.023.

[18] R. S. Mane, S. Pradhan, V. Somkuwar, R. Bhattacharyya, P. C. Ghosh, and N. Jha, "An electron 'donor–acceptor–donor' strategy to activate ZIF67 as a cathode material for fuel cells and zinc ion hybrid supercapacitor," *React. Chem. Eng.*, vol. 8(2023), no. 4, pp. 891–907, doi: 10.1039/D2RE00357K.

[19] J. Qian, F. Sun, and L. Qin, "Hydrothermal synthesis of zeolitic imidazolate framework-67 (ZIF67) nanocrystals," *Mater. Lett.*, vol. 82(2012), pp. 220–223, doi: 10.1016/j.matlet.2012.05.077.

[20] J. Tang *et al.*, "Thermal Conversion of Core–Shell Metal–Organic Frameworks: A New Method for Selectively Functionalized Nanoporous Hybrid Carbon," *J. Am. Chem. Soc.*, vol. 137(2015), no. 4, pp. 1572–1580, doi: 10.1021/ja511539a.

[21] A. F. Gross, E. Sherman, and J. J. Vajo, "Aqueous room temperature synthesis of cobalt and zinc sodalite zeolitic imidizolate frameworks," *Dalton Trans.*, vol. 41(2012), no. 18, pp. 5458–5460, doi: 10.1039/C2DT30174A.

[22] Y. Guo *et al.*, "Effect of Various Pyrolysis Temperatures on ZIF67 Derived Nanoporous Carbons," *Bull. Chem. Soc. Jpn.*, vol. 90(2017), no. 8, pp. 939–942, doi: 10.1246/bcsj.20170138.

[23] J. Tang *et al.*, "Electrochemical determination of dopamine and uric acid using a glassy carbon electrode modified with a composite consisting of a Co(II)-based metalorganic framework (ZIF67) and graphene oxide," *Microchim. Acta*, vol. 185(2018), no. 10, p. 486, doi: 10.1007/s00604-018-3025-x.